Energy distribution analysis of the wavepacket simulations of CH_4 and CD_4 scattering

R. Milot and A. P. J. Jansen

Schuit Institute of Catalysis, ST/SKA, Eindhoven University of Technology
P.O. Box 513, NL-5600 MB Eindhoven, The Netherlands.
E-mail: tgakrm@chem.tue.nl, Tel.:+31-40-2472189, Fax:+31-40-2455054

The isotope effect in the scattering of methane is studied by wavepacket simulations of oriented CH_4 and CD_4 molecules from a flat surface including all nine internal vibrations. At a translational energy up to 96 kJ/mol we find that the scattering is still predominantly elastic, but less so for CD_4. Energy distribution analysis of the kinetic energy per mode and the potential energy surface terms, when the molecule hits the surface, are used in combination with vibrational excitations and the corresponding deformation. They indicate that the orientation with three bonds pointing towards the surface is mostly responsible for the isotope effect in the methane dissociation.

keywords: Computer simulations, Models of surface chemical reaction, Alkanes, Low index single crystal surfaces

1 Introduction

The dissociation of methane on transition metals is an important reaction in catalysis. It is the rate limiting step in steam reforming to produce syngas.[1] It is also prototypical for C–H activation in other processes. A large number of molecular beam experiments in which the dissociation energy was measured as a function of translational energy have already been done on this system.[2–22] These experiments have contributed much to our understanding of the mechanism of the dissociation. Some of them observed that vibrationally hot CH_4 dissociates more readily than cold CH_4, with the energy in the internal vibrations being about as effective as the translational energy in inducing dissociation.[2–8] A more detailed assessment of the importance of the internal vibrations could not be made, because of the large number of internal vibrations. A recent molecular beam experiment with laser excitation of the

ν_3 mode succeeded in measuring a dramatical enhancement of the dissociation on a Ni(100) surface, but it is still much too low to account for the vibrational activation observed in previous studies and indicates that other vibrationally excited modes contribute significantly to the reactivity of thermal samples.[22]

Wavepacket simulations are being used more and more to study the dynamics of this kind of molecule surface reactions. The published wavepacket simulations on the methane dissociation reaction on transition metals have treated the methane molecule always as a diatomic up to now.[23–27] Besides the C–H bond and molecule surface distance, a combination of other coordinates were included, like (multiple) rotations and some lattice motion. None of them have looked at the role of the internal vibrations. Various theoretical studies have obtained reaction pathways and barriers for dissociation by DFT calculations,[28–37] but they cannot explain the role of the vibrational modes in the reaction dynamics either.

A nice way to study reaction dynamics is the use of isotopes. The most recent wavepacket simulation on the dissociation probability of CH_4 and CD_4 showed a semiquantitative agreement with the molecular beam experiments of Ref.[5], except for the isotope effect and the extracted vibrational efficacy.[27] The molecular beam study with laser excitation of the ν_3 asymmetrical stretch mode shows that the incorrect vibrational efficacy is caused by the assumptions in the fit procedure that both stretch modes behaves identical.[22] One of the possible explanation of the incorrect isotope effect can be the role played by the non-included intramolecular vibrations.

In a previous paper we reported on wavepacket simulations that we have done to determine which and to what extent internal vibrations are important for the dissociation of CH_4.[38] We were not able yet to simulate the dissociation including all internal vibrations. Instead we simulated the scattering of methane, for which all internal vibrations can be included, and used the results to deduce consequences for the dissociation. We used model potential energy surfaces (PESs) that have been developed with Ni(111) in mind, but our results should hold for other surfaces as well. At a translational energy up to 96 kJ/mol we found that the scattering is almost completely elastic. Vibrational excitations when the molecule hits the surface and the corresponding deformation depend on generic features of the potential energy surface. In particular, our simulations indicate that for methane to dissociate the interaction of the molecule with the surface should lead to an elongated equilibrium C–H bond length close to the surface.

We have been using the multiconfigurational time-dependent Hartree (MCTDH) method for our wavepacket simulation, because it can deal with a large number of degrees of freedom and with large grids.[39,40] This method has been applied successfully to gas phase reactions and reactions at surfaces.[41–60]

In this paper we report wavepacket simulations of CD_4 scattering including all internal vibrations for fixed orientations, performed on the same model PESs as in our previous paper.[38] Translational motion parallel to the surface and all rotational motion was neglected. No degrees of freedom of the surface were included. Experiments show that coupling with these degrees of freedom is dependent on the metal surface. For example, the observed surface temperature effect are small on Ni[5], but quite large on Pt[7]. As we are only interested in the role of internal vibrations, we have not included degrees of freedom of the surface to keep the simulations as simple as possible. We will discuss the vibrational excitation and the deformation of the CD_4 molecule when it hits the surface and compare it with CH_4. Later on we will look at the energy distribution of the kinetic energy per mode and the potential energy in some terms of the PES with the elongated equilibrium bond length close to the surface for both isotopes. The transfer of translational kinetic energy towards vibrational kinetic energy gives an indication about the dissociation probability, since vibrational kinetic energy helps in overcoming the dissociation barrier. It gives a better idea too about which modes are essential to include in a more accurate wavepacket simulation of methane dissociation. After that we will discuss the implications of this for the dissociation and give a summary with some general conclusions.

2 Computational details

2.1 The Potential Energy Surfaces

We used for the scattering of CD_4 the same model PESs as we did for CH_4. Since we expressed the PES in mass-weighted coordinated the parameters in the PESs for CD_4 differs from CH_4. We will now give an overview of our model PESs and the corresponding parameters for CD_4. The parameters of CH_4 for these PESs were already given in Ref. [38], where also more detailed information about our assumptions and contour plots of some cross-section of the model PESs can be found.

The PESs we used can all be written as

$$V_{\text{total}} = V_{\text{intra}} + V_{\text{surf}}, \tag{1}$$

where V_{intra} is the intramolecular PES and V_{surf} is the repulsive interaction with the surface. For the V_{intra} we looked at four different types of PESs. The V_{intra} include also for two types changes in the intramolecular potential due to interactions with the surface.

2.1.1 A harmonic potential

The first one is completely harmonic. We have used normal mode coordinates for the internal vibrations, because these are coupled only very weakly. In the harmonic approximation this coupling is even absent so that we can write $V_{\rm intra}$ as

$$V_{\rm intra} = V_{\rm harm} = \frac{1}{2}\sum_{i=2}^{10} k_i X_i^2, \tag{2}$$

the summation is over the internal vibrations, X_i's are mass-weighted displacement coordinates and k_i are mass-weighted force constants. (see Table 1 for definitions and values); (X_1 is the mass-weighted overall translation along the surface normal).[61] The force constants have been obtained by fitting them on the experimental vibrational frequencies of CH_4 and CD_4.[62,63]

We have assumed that the repulsive interaction with the surface is only through the deuterium atoms that point towards the surface. We take the z-axis as the surface normal. In this case the surface PES is given by

$$V_{\rm surf} = \frac{A}{N_D}\sum_{i=1}^{N_D} e^{-\alpha z_i}, \tag{3}$$

where N_D is the number of deuteriums that points towards the surface, α=1.0726 atomic units and A=6.4127 Hartree. These parameters are chosen to give the same repulsion as the PES that has been used in an MCTDH wavepacket simulation of CH_4 dissociation.[26]

If we write $V_{\rm surf}$ in terms of normal mode coordinates, then we obtain for one deuterium pointing towards the surface

$$V_{\rm surf} = A e^{-\alpha_1 X_1} e^{-\alpha_2 X_2} e^{-\alpha_3 X_3} e^{-\alpha_4 X_4}, \tag{4}$$

where A as above, and α's as given in Table 2. X_2, X_3 and X_4 correspond all to a_1 modes of the C_{3v} symmetry (see Fig. 1). There is no coupling between the modes X_5 to X_{10} in the $V_{\rm surf}$ part of the PES, which are all e modes of the C_{3v} symmetry.

For two deuteriums we obtain

$$\begin{aligned} V_{\rm surf} = A\ & e^{-\alpha_1 X_1} e^{-\alpha_2 X_2} e^{-\alpha_3 X_3} e^{-\alpha_4 X_4} e^{-\alpha_5 X_5} \\ & \times \frac{1}{2}\Big[\ e^{\beta_3 X_7} e^{-\beta_3 X_8} e^{\beta_5 X_9} e^{-\beta_5 X_{10}} \\ & \quad + e^{-\beta_3 X_7} e^{\beta_3 X_8} e^{-\beta_5 X_9} e^{\beta_5 X_{10}}\Big], \end{aligned} \tag{5}$$

with A again as above, α's and β's as given in Table 2. X_2, X_3, X_4 and X_5 correspond all to a_1 modes of C_{2v}. X_7, X_8, X_9 and X_{10} correspond to b_1 and b_2 modes of C_{2v}. X_6 corresponds to the a_2 mode of C_{2v} and has no coupling with the other modes in $V_{\rm surf}$.

For three deuteriums we obtain

$$\begin{aligned} V_{\rm surf} = A\ & e^{-\alpha_1 X_1} e^{-\alpha_2 X_2} e^{-\alpha_3 X_3} e^{-\alpha_4 X_4} \\ & \times \frac{1}{3}\Big[\ e^{\beta_1 X_5} e^{\beta_2 X_6} e^{-\beta_3 X_7} e^{\beta_4 X_8} e^{\beta_5 X_9} e^{-\beta_6 X_{10}} \\ & \quad + e^{\beta_1 X_5} e^{-\beta_2 X_6} e^{-\beta_3 X_7} e^{-\beta_4 X_8} e^{\beta_5 X_9} e^{\beta_6 X_{10}} \\ & \quad + e^{-2\beta_1 X_5} e^{2\beta_3 X_7} e^{-2\beta_5 X_9}\Big], \end{aligned} \tag{6}$$

with A again as above, α's and β's as given in Table 2. X_2, X_3 and X_4 corresponds to a_1 modes in the C_{3v} symmetry (see Fig. 1). Because these last six coordinates correspond to degenerate e modes of the C_{3v} symmetry, the β parameters are not unique.

2.1.2 An anharmonic intramolecular potential

Even though we do not try to describe the dissociation of methane in this and our previous paper, we do want to determine which internal vibration might be important for this dissociation. The PES should at least allow the molecule to partially distort as when dissociating. The harmonic PES does not do this. A number of changes have therefor been made. The first is that we have describe the C–D bond by a Morse PES.

$$V_{\rm Morse} = D_e \sum_{i=1}^{4} \Big[1 - e^{-\gamma \Delta r_i}\Big]^2, \tag{7}$$

where $D_e = 0.1828$ Hartree (the dissociation energy of methane in the gas-phase) and Δr_i the change in bond length from the equilibrium distance. γ was calculated by equating the second derivatives along one bond of the harmonic and the Morse PES. If we transform Eq. (7) back into normal mode coordinates, we obtain

$$V_{\rm Morse} = D_e \sum_{i=1}^{4} \Big[1 - e^{\gamma_{i2} X_2} e^{\gamma_{i3} X_3} e^{\gamma_{i4} X_4} e^{\gamma_{i7} X_7} e^{\gamma_{i8} X_8} e^{\gamma_{i9} X_9} e^{\gamma_{i,10} X_{10}}\Big]^2, \tag{8}$$

with D_e as above. γ's are given in Tables 3 and 4. Note that, although we have only changed the PES of the bond lengths, the ν_4 umbrella modes are also affected. This is because these modes are not only bending, but also contain some changes of bond length.

The new intramolecular PES now becomes

$$V_{\text{intra}} = V_{\text{harm}} + V_{\text{Morse}} - V_{\text{corr}}, \tag{9}$$

where V_{harm} is as given in Eq. (2) and V_{corr} is the quadratic part of V_{Morse}, which is already in V_{harm}.

2.1.3 Intramolecular potential with weakening C–D bonds

When the methane molecule approach the surface the overlap of substrate orbitals and anti-bonding orbitals of the molecule weakens the C–D bonds. We want to include this effect for the C–D bonds of the deuteriums pointing towards the surface. We have redefined the V_{Morse} given in Eq. (8) and also replace it in Eq. (9). A sigmoidal function is used to switch from the gas phase C–D bond to a bond close to the surface. We have used the following, somewhat arbitrary, approximations. (i) The point of inflection should be at a reasonable distance from the surface. It is set to the turnaround point for a rigid methane molecule with translation energy 93.2 kJ/mol plus twice the fall-off distance of the interaction with the surface. (ii) The depth of the PES of the C–D bond is 480 kJ/mol in the gas phase, but only 93.2 kJ/mol near the surface. The value 93.2 kJ/mol corresponds to the height of the activation barrier used in our dissociation.[26] (iii) The exponential factor is the same as for the interaction with the surface.

If we transform to normal-mode coordinates for the particular orientations, we then obtain

$$V_{\text{weak}} = D_e \sum_{i=1}^{4} W_i \Big[1 - e^{\gamma_{i2}X_2} e^{\gamma_{i3}X_3} e^{\gamma_{i4}X_4} e^{\gamma_{i7}X_7} e^{\gamma_{i8}X_8} e^{\gamma_{i9}X_9} e^{\gamma_{i,10}X_{10}}\Big]^2, \tag{10}$$

where $W_i = 1$ for non-interacting bonds and

$$W_i = \frac{1 + \Omega e^{-\alpha_1 X_1 + \omega}}{1 + e^{-\alpha_1 X_1 + \omega}} \tag{11}$$

for the interacting bonds pointing towards the surface. α_1 is as given in Table 2, γ's are given in Tables 3 and 4, $\Omega = 1.942 \cdot 10^{-1}$ and $\omega = 7.197$.

2.1.4 Intramolecular potential with elongation of the C–D bonds

A weakened bond generally has not only a reduced bond strength, but also an increased bond length. We include the effect of the elongation of the C–D bond length of the deuteriums that point towards the surface due to interactions

with the surface. We have redefined the $V_{\rm Morse}$ given in Eq. (8) and also replace it in Eq. (9) for this type of PES. We have used the following approximations: (i) The transition state, as determined by Ref. [30] and [64], has a C–H bond that is 0.54 Å longer than normal. This elongation should occur at the turn around point for a rigid methane molecule with a translation energy of 93.2 kJ/mol. (ii) The exponential factor is again the same as for the interaction with the surface.

If we transform to normal-mode coordinates for the particular orientations, then we obtain

$$V_{\rm shift} = D_e \sum_{i=1}^{4} \left[1 - e^{\gamma_{i2}X_2} e^{\gamma_{i3}X_3} e^{\gamma_{i4}X_4} e^{\gamma_{i7}X_7} e^{\gamma_{i8}X_8} e^{\gamma_{i9}X_9} e^{\gamma_{i,10}X_{10}} \exp[S_i e^{-\alpha_1 X_1}]\right]^2, \quad (12)$$

where α_1 is as given in Table 2, γ's are given in Tables 3 and 4. For orientation with one deuterium towards the surface we obtain; $S_1 = 2.942 \cdot 10^2$ and $S_2 = S_3 = S_4 = 0$, with two deuteriums; $S_1 = S_2 = 0$ and $S_3 = S_4 = 1.698 \cdot 10^2$, and with three deuteriums; $S_1 = 0$ and $S_2 = S_3 = S_4 = 2.942 \cdot 10^2$.

2.2 Initial States

The exact wave-function of a D-dimensional system, is expressed in the MCTDH approximation by the form

$$\Psi_{\rm MCTDH}(q_1, \ldots, q_D; t) = \sum_{n_1 \ldots n_D} c_{n_1 \ldots n_D}(t)\, \psi^{(1)}_{n_1}(q_1; t) \ldots \psi^{(D)}_{n_D}(q_D; t). \quad (13)$$

All initial states in the simulations start with the vibrational ground state. The initial translational part $\psi^{(\rm tr)}$ is represented by a Gaussian wave-packet,

$$\psi^{(\rm tr)}(X_1) = (2\pi\sigma^2)^{-1/4} \exp\left[-\frac{(X_1 - X_0)^2}{4\sigma^2} + iP_1X_1\right], \quad (14)$$

where σ is the width of the wave-packet (we used $\sigma = 320.248$ atomic units), X_0 is the initial position (we used $X_0 = 11\sigma$, which is far enough from the surface to observe no repulsion) and P_1 is the initial momentum. Since we used mass-weighted coordinates the Gaussian wavepacket are identical for CD_4 and CH_4. We performed simulations in the energy range of 32 to 96 kJ/mol. We here present only the results of 96 kJ/mol (equivalent to $P_1 = -0.2704$ atomic units), because they showed the most obvious excitation probabilities for $V_{\rm Morse}$. We used seven natural single-particle states, 512 grid points and a grid-length of 15σ for the translational coordinate. With this grid-width we can perform simulation with a translational energy up to 144 kJ/mol.

Gauss-Hermite discrete-variable representations (DVR)[65] were used to represent the wavepackets of the vibrational modes. We used for all simulations of CD_4 the same number of DVR points as for CH_4, which was 5 DVR points for the ν_2 bending modes and 8 DVR points for the ν_4 umbrella, ν_3 asymmetrical stretch, and ν_1 symmetrical stretch mode for an numerical exact integration, except for the simulations with V_{shift}, where we used 16 DVR points for the ν_1 symmetrical stretch mode, because of the change in the equilibrium position.

Also the same configurational basis was used for both isotopes. We did the simulation with one bond pointing towards the surface in eight dimensions, because the ν_2 bending modes X_5 and X_6 do not couple with the other modes. We needed four natural single-particle states for modes X_2, X_3 and X_4, and just one for the others. So the number of configurations was $7^1 \cdot 4^3 \cdot 1^4 = 448$. The simulation with two bonds pointing towards the surface was performed in nine dimensions. One of the ν_2 bending mode (X_6) does not couple with the other modes, but for the other mode X_5 we needed four natural single-particle states. The number of configurations was $7^1 \cdot 4^4 \cdot 1^4 = 1792$, because we needed the same number of natural single-particle states as mentioned above for the other modes. We needed ten dimensions to perform the simulation with three bonds pointing towards the surface. We used here one natural single-particle state for the modes X_5 to X_{10} and four natural single-particle states for X_2 to X_4, which gave us $7^1 \cdot 4^3 \cdot 1^6 = 448$ configurations.

3 Results and Discussion

3.1 Excitation probabilities and structure deformation of CD_4

The scattering probabilities for CD_4 are predominantly elastic, as we also found in our previous simulations of CH_4 scattering.[38] The elastic scattering probability is larger than 0.99 for all orientation of the PESs with V_{Morse} and V_{weak} at a translational energy of 96 kJ/mol. For the PES with V_{shift} we observe an elastic scattering probability of 0.981 for the orientation with one, 0.955 with two and 0.892 with three deuteriums pointing towards the surface. This is lower than we have found for CH_4, which is 0.956 for the orientation with three hydrogens pointing towards the surface and larger than 0.99 for the others. The higher inelastic scattering probabilities of CD_4 was expected, because the force constants k_i of CD_4 are decreased up to 50% with respect to those of CH_4 and the translational surface repulsion fall-off differs only little.

When we look at the excitation probabilities at the surface for the PES with V_{Morse} and V_{weak}, then we observe generally an increase for CD_4 compared with CH_4, except for the ν_4 umbrella mode in the orientation with two bond point-

ing towards the surface. Relevant differences in the structure deformations are observed only in the bond angles, which are increased for CD_4 in the orientations with one and three bonds pointing towards the surface. The bond angle deformation of the angle between the bonds pointing towards the surface in the orientation with two bonds pointing towards the surface is decreased for CD_4. We observe again that the PES with V_{weak} gives larger structure deformations than the PES with V_{Morse}, but the differences are smaller for CD_4 than CH_4.

For the PES with V_{shift} we do not observe this effect on the bond angle deformation. The bond angle deformation for the orientation with two and three deuteriums pointing towards the surface is the same as for CH_4 and it is just $0.1°$ less for the bond angle at the surface side in the orientation with one deuterium pointing towards the surface. The excitation probabilities (see Table 5) for the ν_2 bending and ν_4 umbrella modes become higher for all orientations for CD_4, which is necessary for getting the same bond angle deformations as CH_4.

The changes in the bond distances for the orientations with one and two bonds pointing towards the surface is for CD_4 almost the same as for CH_4. For the orientation with three bonds pointing towards the surface, we found that the maximum bond lengthening of the bonds on the surface side was 0.032 Å less for CD_4 than CH_4. We also found that the bond shortening of the bond pointing away from the surface is 0.010 Å more for CD_4. These are only minimal differences, which also only suggest that the bond deformation for CD_4 has been influenced slightly more by the ν_3 asymmetrical stretch mode than the ν_1 symmetrical stretch mode. The observed excitation probabilities for these modes do not contradict this, but are not reliable enough for hard conclusions because of their high magnitude. It is also not clear, beside of this problem, what they really represent. Is the excitation caused by a different equilibrium position of the PES at the surface in a mode or is it caused by extra energy in this mode? To answer these questions we decided to do an energy distribution analysis during the scattering for both isotopes.

3.2 Energy distribution in CH_4 and CD_4

The energy distribution analysis is performed by calculating the expectation values of the important term of the Hamiltonian H for the wave-function $\Psi(t)$ at a certain time t during the scattering of CD_4 and CH_4 for all presented orientations in this and our previous paper.[38] We will present here only the results of the PES with V_{shift}, because it is the only model PES for which the energy distribution analysis is relevant for the discussion of the dissociation hypotheses later on.

We can obtain good information about the energy distribution per mode by looking at the kinetic energy expectation values $\langle\Psi(t)|T_j|\Psi(t)\rangle$ per mode j (see Table 6), because the kinetic energy operators T_j have no cross terms like the PESs have. When we discuss the kinetic energy of a mode we normally refer to the a_1 mode of the C_{3v} or C_{2v} symmetry, because in these modes we have observed the highest excitation probabilities and the change in kinetic energy in the other modes is generally small.

By looking at the expectation values of some terms of the PES $\langle\Psi(t)|V_{\text{term}}|\Psi(t)\rangle$ (see Table 7), we obtain information about how the kinetics of the scattering is driven by the PES. The V_{surf} PES [see Eqs. (4), (5) and (6)] is the surface hydrogen/deuterium repulsion for a given orientation. $V_{\text{harm}}(\nu_2)$ and $V_{\text{harm}}(\nu_4)$ [see Eq. (2)] are the pure harmonic terms of the intramolecular PES of the a_1 modes in the C_{3v} and C_{2v} symmetry corresponding to a ν_2 bending and ν_4 umbrella modes, respectively. The pure harmonic correction terms of V_{corr} [see Eq. (9)] are included in them. $V_{\text{bond}}(R_{\text{up}})$ and $V_{\text{bond}}(R_{\text{down}})$ are the potential energy in a single C–H or C–D bond pointing respectively towards and away from the surface, and they give the expectation value of one bond term of V_{shift} [see Eq. (12)]. All given expectation values are the maximum deviation of the initial values, which effectively means the values at the moment the molecule hits the surface.

The largest changes in expectation values are, of course, in the kinetic energy of the translational mode. The translational kinetic energy does not become zero as we should expect in classical dynamics. The loss of translational kinetic energy is primary absorbed by the V_{surf} terms of the PESs. The expectation values of the V_{surf} terms show the ability of the hydrogens or deuteriums to come close to the metal surface, since in real space their exponential fall-offs are the same for both isotopes. For a rigid molecule the sum of the translational kinetic energy and V_{surf} should be constant, so all deviations of this sum have to be found back in the intramolecular kinetic energy and other PES terms.

We observe that both the minimum in the translational kinetic energy and the maximum in the V_{surf} terms were higher for CH_4 than CD_4, so we have to find more increase in energy in the intramolecular modes and PES terms for CD_4 than CH_4. We indeed do so and that can be one of the reasons we found higher inelastic scatter probabilities for CD_4 for the PES with V_{shift} .

For the orientations with one and two bonds pointing towards the surface we observe a large increase of the kinetic energy in the ν_3 asymmetrical stretch mode. If we compare this with the excitation probabilities, we find that the kinetic energy analysis gives indeed a different view on the dynamics. For the orientation with two bond pointing towards the surface we have found for both isotopes very high excitation probabilities in the ν_1 and ν_3 stretch modes. We know now from the kinetic energy distribution that for the ν_1 symmetrical

stretch mode the high excitation probability is caused by the change of the equilibrium position of the ν_1 mode in the PES and that for the ν_3 stretch mode probably the PES also has become narrower.

For the orientation with three bonds pointing towards the surface we also obtain an large increase of the kinetic energy of the ν_3 asymmetrical stretch mode, but we also find an even larger increase in the kinetic energy of the ν_1 symmetrical stretch mode. The total kinetic energy was extremely large, because the kinetic energy of the translational mode becomes also much larger than for the other orientations. Because of this the V_{surf} terms had to be around twice as low as for the other orientations.

All $V_{\mathrm{bond}}(R_{\mathrm{up}})$ terms become lower compared to the initial value, especially in the orientation with two bond pointing towards the surface. In the orientation with one bond pointing towards the surface, the $V_{\mathrm{bond}}(R_{\mathrm{down}})$ term became higher. This is caused by the repulsion of V_{surf} in the direction of the bond. The increase of this PES term value is higher for CD_4 than CH_4.

In the orientation with three bond pointing towards the surface we also observe a higher $V_{\mathrm{bond}}(R_{\mathrm{down}})$ value, with also the highest increase for CD_4. In relation with the somewhat shorter bond distance for the R_{down} of CD_4 compared with CH_4, which was also a bit lower compared with the other orientations, we know now that the hydrogens and especially the deuterium have problems in following the minimum energy path of the PES with V_{shift} during the scattering dynamics. This leads to higher kinetic energy in the vibrational modes, which results in more inelastic scattering.

The $V_{\mathrm{harm}}(\nu_2)$ term increases in respect to the initial value, but not as much as the increase of the $V_{\mathrm{harm}}(\nu_4)$ is for the orientation with two bonds pointing towards the surface. The values of $V_{\mathrm{harm}}(\nu_4)$ for CD_4 are even higher than for CH_4. We observe also a larger increase of the kinetic energy in the ν_4 umbrella mode for CD_4 than for CH_4. So although there is somewhat more energy transfer to the vibrational modes for CD_4 than CH_4, this extra vibrational energy is absorbed especially in the ν_4 umbrella mode of CD_4.

3.3 Dissociation hypotheses

We like now to discuss some possible implications of the scattering simulation for the isotope effect on the dissociation of methane. In our previous paper we have already drawn some conclusions about the possible reaction mechanism and which potential type would be necessary for dissociation.[38] We found the direct breaking of a single C–H bond in the initial collision more reasonable than the splats model with single bond breaking after an intermediary Ni–C bond formation as suggested by Ref. [4], because the bond angle deformations

seems to small to allow a Ni–C to form. From the simulations with CD_4 we can draw the same conclusions. The PES with V_{shift} gives the same angle deformations for both isotopes, which is not sufficient for the splats model. The other potentials give higher bond angle deformations for the orientation with three deuteriums pointing towards the surface. If the Ni–C bond formation would go along this reaction path, then the dissociation of CD_4 should be even more preferable than CH_4, which is not the case. So we only have to discuss the implication of the scattering simulation for the dissociation probabilities of CH_4 and CD_4 for a direct breaking of a single bond reaction mechanism. This reaction mechanism can be influenced by what we will call a direct or an indirect effect.

A direct effects is the expected changes in the dissociation probability between CH_4 and CD_4 for a given orientation. Since we expect that we need for dissociation a PES with an elongation of the bonds pointing towards the surface, we only have to look at the isotope effect in the simulation for the PES with V_{shift} for different orientations to discuss some direct effect. It is clear from our simulations that the bond lengthening of CD_4 is smaller than CH_4 for the orientation with three bonds pointing towards the surface. If this orientation has a high contribution to the dissociation of methane, then this can be the reason of the higher dissociation probability of CH_4. In this case our simulations also explain why Ref.[27] did not observe a high enough isotope effect in the dissociation probability of their simulation with CH_4 and CD_4 modelled by a diatomic, because we do not observe a change in bond lengthening between the isotopes for the orientation with one bond pointing towards the surface.

The orientation with three bonds pointing towards the surface is also the orientation with the highest increase of the total vibrational kinetic energy for the PES with V_{shift}, because the energy distribution analysis shows besides an high increase of the kinetic energy in the ν_3 asymmetrical stretch mode also an high increase in the ν_1 symmetrical stretch mode. Since vibrational kinetic energy can be used effectively to overcome the dissociation barrier, the orientation with three bonds indicates to be a more preferable orientation for dissociation. Moreover the relative difference in kinetic energy between both isotopes is for the ν_1 stretch mode larger than for the ν_3 stretch mode. If the kinetic energy in the ν_1 stretch mode contributes significantly to overcoming the dissociation barrier, then it is another explanation for the low isotope effect in Ref.[27].

An indirect effect is the expected changes in the dissociation probability between CH_4 and CD_4 through changes in the orientations distribution caused by the isotope effect in the vibrational modes. This can be the case if the favourable orientation for dissociation is not near the orientation with three bonds pointing towards the surface, but more in a region where one or two bonds pointing towards the surface. These orientations do not show a large

difference in deformation for the PES with V_{shift}. We can not draw immediate conclusion about the indirect effect from our simulations, since we did not include rotational motion, but our simulation show that an indirect isotope effect can exist. For the PES with V_{Morse} in the orientation with three bonds pointing towards the surface, we observe that CD_4 is able to come closer to the surface than CH_4. So this rotational orientation should be more preferable for CD_4 than for CH_4. On the other hand, if the PES is in this orientation more like V_{shift} the dissociation probability in other orientation can be decreased for CD_4 through higher probability in inelastic scattering channels.

So for both effects the behaviour of the orientation with three bonds pointing towards the surface seems to be essential for a reasonable description of the dissociation mechanism of methane. A wavepacket simulation of methane scattering including one or more rotational degrees of freedom and the vibrational stretch modes will be a good starting model to study the direct and indirect effects, since most of the kinetic energy changes are observed in the stretch modes and so the bending and umbrella modes are only relevant with accurate PESs. Eventually dissociation paths can be introduced in the PES along one or more bonds.

Beside of our descriptions of the possible isotopes effect for the dissociation extracted of the scatter simulations we have to keep in mind that also a tunneling mechanism can be highly responsible for the higher observed isotope effect in the experiment and that a different dissociation barrier in the simulations can enhance this effect of tunneling.

4 Conclusions

The scattering is in all cases predominantly elastic. However, the observed inelastic scattering is higher for CD_4 compared with previous simulation on CH_4 for the PES with an elongated equilibrium bond length close to the surface. When the molecule hits the surface, we observe in general a higher vibrational excitation for CD_4 than CH_4. The PES with an elongated equilibrium bond length close to the surface gives for both isotopes almost the same deformations, although we observe a somewhat smaller bond lengthening for CD_4 in the orientation with three bonds pointing towards the surface. The other model PESs show differences in the bond angle deformations and in the distribution of the excitation probabilities of CD_4 and CH_4, especially for the PES with only an anharmonic intramolecular potential.

Energy distribution analysis contributes new information on the scattering dynamics. A higher transfer of translational energy towards vibrational kinetic energy at the surface results in higher inelastic scattering. The highest increase

of vibrational kinetic energy is found in the ν_3 asymmetrical stretch modes for all orientations and also in the ν_1 symmetrical stretch mode for the orientation with three bonds pointing towards the surface, when the PES has an elongated equilibrium bond length close to the surface.

Our simulations give an indication that the isotope effect in the methane dissociation is caused mostly by the difference in the scattering behaviour of the molecule in the orientation with three bonds pointing towards the surface. At least multiple vibrational stretch modes should be included for a reasonable description of isotope effect in the methane dissociation reaction.

Acknowledgments

This research has been financially supported by the Council for Chemical Sciences of the Netherlands Organization for Scientific Research (CW-NWO). This work has been performed under the auspices of NIOK, the Netherlands Institute for Catalysis Research, Lab Report No. TUE-99-5-02.

References

[1] J. P. Van Hook, Catal. Rev. Sci. Eng. 21 (1980) 1.

[2] C. T. Rettner, H. E. Pfnür and D. J. Auerbach, Phys. Rev. Lett. 54 (1985) 2716.

[3] C. T. Rettner, H. E. Pfnür and D. J. Auerbach, J. Chem. Phys. 84 (1986) 4163.

[4] M. B. Lee, Q. Y. Yang and S. T. Ceyer, J. Chem. Phys. 87 (1987) 2724.

[5] P. M. Holmbad, J. Wambach and I. Chorkendorff, J. Chem. Phys. 102 (1995) 8255.

[6] J. H. Larsen, P. M. Holmblad and I. Chorkendorff, J. Chem. Phys. 110 (1999) 2637.

[7] A. C. Luntz and D. S. Bethune, J. Chem. Phys. 90 (1989) 1274.

[8] A. V. Walker and D. A. King, Phys. Rev. Lett. 82 (1999) 5156.

[9] M. B. Lee, Q. Y. Yang, S. L. Tang and S. T. Ceyer, J. Chem. Phys. 85 (1986) 1693.

[10] S. T. Ceyer, J. D. Beckerle, M. B. Lee, S. L. Tang, Q. Y. Yang and M. A. Hines, J. Vac. Sci. Techmol. A 5 (1987) 501.

[11] J. D. Beckerle, A. D. Johnson, Q. Y. Yang and S. T. Ceyer, J. Chem. Phys. 91 (1989) 5756.

[12] P. M. Holmbad, J. H. Larsen and I. Chorkendorff, J. Chem. Phys. 104 (1996) 7289.

[13] G. R. Schoofs, C. R. Arumanayagam, M. C. McMaster and R. J. Madix, Surf. Sci. 215 (1989) 1.

[14] A. V. Hamza and R. J. Madix, Surf. Sci. 179 (1987) 25.

[15] M. Valden, N. Xiang, J. Pere and M. Pessa, App. Surf. Sci. 99 (1996) 83.

[16] M. Valden, J. Pere, N. Xiang and M. Pessa, Chem. Phys. Lett. 257 (1996) 289.

[17] R. W. Verhoef, D. Kelly, C. B. Mullins and W. H. Weinberg, Surf. Sci. 287 (1993) 94.

[18] R. W. Verhoef, D. Kelly, C. B. Mullins and W. H. Weinberg, Surf. Sci. 311 (1994) 196.

[19] R. W. Verhoef, D. Kelly, C. B. Mullins and W. H. Weinberg, Surf. Sci. 325 (1995) 93.

[20] D. C. Seets, M. C. Wheeler and C. B. Mullins, J. Chem. Phys. 107 (1997) 3986.

[21] D. C. Seets, C. T. Reeves, B. A. Ferguson, M. C. Wheeler and C. B. Mullins, J. Chem. Phys. 107 (1997) 10229.

[22] L. B. F. Juurlink, P. R. McCabe, R. R. Smith, C. L. DiCologero and A. L. Utz, Phys. Rev. Lett. 83 (1999) 868.

[23] A. C. Luntz and J. Harris, Surf. Sci. 258 (1991) 397.

[24] A. C. Luntz and J. Harris, J. Vac. Sci. A 10 (1992) 2292.

[25] A. C. Luntz, J. Chem. Phys. 102 (1995) 8264.

[26] A. P. J. Jansen and H. Burghgraef, Surf. Sci. 344 (1995) 149.

[27] M.-N. Carré and B. Jackson, J. Chem. Phys. 108 (1998) 3722.

[28] H. Yang and J. L. Whitten, J. Chem. Phys. 96 (1992) 5529.

[29] H. Burghgraef, A. P. J. Jansen and R. A. van Santen, J. Chem. Phys. 98 (1993) 8810.

[30] H. Burghgraef, A. P. J. Jansen and R. A. van Santen, Chem. Phys. 177 (1993) 407.

[31] H. Burghgraef, A. P. J. Jansen and R. A. van Santen, J. Chem. Phys. 101 (1994) 11012.

[32] H. Burghgraef, A. P. J. Jansen and R. A. van Santen, Surf. Sci. 324 (1995) 345.

[33] P. Kratzer, B. Hammer and J. K. Nørskov, J. Chem. Phys. 105 (1996) 5595.

[34] C.-T. Au, M.-S. Liao and C.-F. Ng, Chem. Phys. Lett. 267 (1997) 44.

[35] M.-S. Liao, C.-T. Au and C.-F. Ng, Chem. Phys. Lett. 272 (1997) 445.

[36] C.-T. Au, C.-F. Ng and M.-S. Liao, J. Catal. 185 (1999) 12.

[37] H. Bengaard, I. Alstrup, I. Chorkendorff, S. Ullmann, J. R. Rostrup-Nielsen and J. K. Nørskov, J. Catal. 187 (1999) 238.

[38] R. Milot and A. P. J. Jansen, J. Chem. Phys. 109 (1998) 1966.

[39] U. Manthe, H.-D. Meyer and L. S. Cederbaum, J. Chem. Phys. 97 (1992) 3199.

[40] A. P. J. Jansen, J. Chem. Phys. 99 (1993) 4055.

[41] U. Manthe, H.-D. Meyer and L. S. Cederbaum, J. Chem. Phys. 97 (1992) 9062.

[42] U. Manthe and A. D. Hammerich, Chem. Phys. Lett. 211 (1993) 7.

[43] A. D. Hammerich, U. Manthe, R. Kosloff, H.-D. Meyer and L. S. Cederbaum, J. Chem. Phys. 101 (1994) 5623.

[44] J.-Y. Fang and H. Guo, J. Chem. Phys. 101 (1994) 5831.

[45] J.-Y. Fang and H. Guo, Chem. Phys. Lett. 235 (1995) 341.

[46] J.-Y. Fang and H. Guo, J. Chem. Phys. 102 (1995) 1944.

[47] L. Liu, J.-Y. Fang and H. Guo, J. Chem. Phys. 102 (1995) 2404.

[48] A. Capellini and A. P. J. Jansen, J. Chem. Phys. 104 (1996) 3366.

[49] M. Ehara, H.-D. Meyer and L. S. Cederbaum, J. Chem. Phys. 105 (1996) 8865.

[50] G. A. Worth, H.-D. Meyer and L. S. Cederbaum, J. Chem. Phys. 105 (1996) 4412.

[51] A. Jäckle and H.-D. Meyer, J. Chem. Phys. 105 (1996) 6778.

[52] U. Manthe and F. Matzkies, Chem. Phys. Lett. 252 (1996) 71.

[53] F. Matzkies and U. Manthe, J. Chem. Phys. 106 (1997) 2646.

[54] T. Gerdts and U. Manthe, J. Chem. Phys. 107 (1997) 6584.

[55] M. H. Beck and H.-D. Meyer, Z. Phys. D 42 (1997) 113.

[56] A. Jäckle and H.-D. Meyer, J. Chem. Phys. 109 (1998) 2614.

[57] A. Jäckle and H.-D. Meyer, J. Chem. Phys. 109 (1998) 3772.

[58] G. A. Worth, H.-D. Meyer and L. S. Cederbaum, J. Chem. Phys. 109 (1998) 3518.

[59] F. Matzkies and U. Manthe, J. Chem. Phys. 110 (1999) 88.

[60] A. Jäckle, M.-C. Heitz and H.-D. Meyer, J. Chem. Phys. 110 (1999) 241.

[61] E. B. Wilson, J. C. Decius and P. C. Cross, Molecular Vibrations. The Theory of Infrared and Raman Spectra. (McGraw-Hill, London, 1955).

[62] D. L. Gray and A. G. Robiette, Mol. Phys. 37 (1979) 1901.

[63] T. J. Lee, J. M. L. Martin and P. R. Taylor, J. Chem. Phys. 102 (1995) 254.

[64] H. Burghgraef, A. P. J. Jansen and R. A. van Santen, Faraday Discuss. 96 (1993) 337.

[65] J. C. Light, I. P. Hamilton and J. V. Lill, J. Chem. Phys. 82 (1985) 1400.

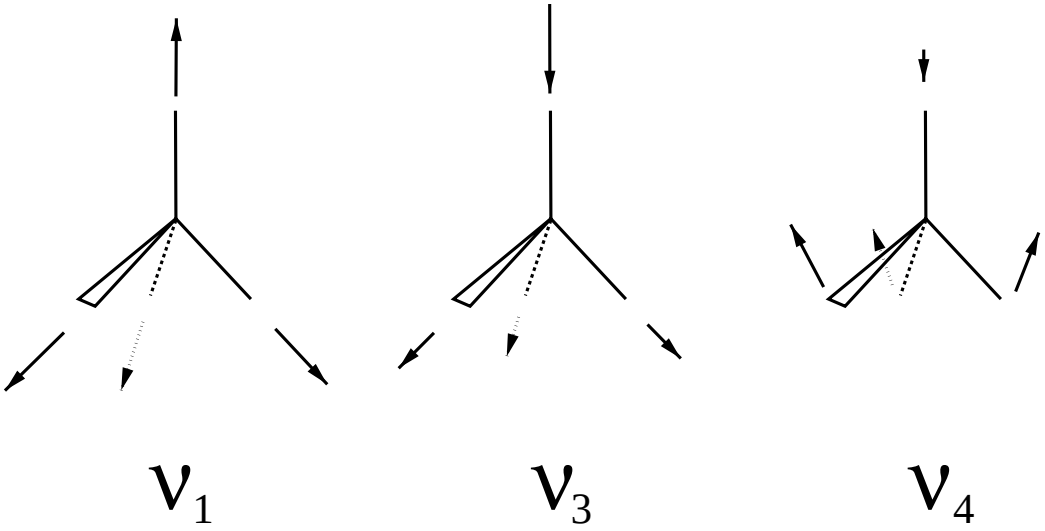

Fig. 1. The a_1 vibrational normal modes in the C_{3v} symmetry; ν_1 symmetrical stretch (X_2), ν_3 asymmetrical stretch (X_4), and ν_4 umbrella (X_3).

Table 1
Overview of the relations between the mass-weighted coordinates X_i; the force constants k_i (in atomic units) for CD_4, the designation, and the symmetry in T_d, C_{3v} and C_{2v}.

i	k_i	designation	T_d	C_{3v}	C_{2v}
1		translation	t_2	a_1	a_1
2	$8.897 \cdot 10^{-5}$	ν_1; symmetrical stretch	a_1	a_1	a_1
3	$2.008 \cdot 10^{-5}$	ν_4; umbrella	t_2	a_1	a_1
4	$1.060 \cdot 10^{-4}$	ν_3; asymmetrical stretch	t_2	a_1	a_1
5	$2.447 \cdot 10^{-5}$	ν_2; bending	e	e	a_1
6	$2.447 \cdot 10^{-5}$	ν_2; bending	e	e	a_2
7	$2.008 \cdot 10^{-5}$	ν_4; umbrella	t_2	e	b_1
8	$2.008 \cdot 10^{-5}$	ν_4; umbrella	t_2	e	b_2
9	$1.060 \cdot 10^{-4}$	ν_3; asymmetrical stretch	t_2	e	b_1
10	$1.060 \cdot 10^{-4}$	ν_3; asymmetrical stretch	t_2	e	b_2

Table 2
α and β values (in atomic units) of V_{surf} for CD_4 with one, two or three deuteriums pointing towards the surface [see Eqs. (4), (5) and (6)].

	one	two	three
α_1	$5.617 \cdot 10^{-3}$	$5.617 \cdot 10^{-3}$	$5.617 \cdot 10^{-3}$
α_2	$8.882 \cdot 10^{-3}$	$5.128 \cdot 10^{-3}$	$2.960 \cdot 10^{-3}$
α_3	$4.703 \cdot 10^{-3}$	$-4.614 \cdot 10^{-3}$	$-7.720 \cdot 10^{-3}$
α_4	$-1.353 \cdot 10^{-2}$	$-5.103 \cdot 10^{-3}$	$-2.295 \cdot 10^{-3}$
α_5		$-7.252 \cdot 10^{-3}$	
β_1			$4.187 \cdot 10^{-3}$
β_2			$7.252 \cdot 10^{-3}$
β_3		$4.659 \cdot 10^{-3}$	$2.196 \cdot 10^{-3}$
β_4			$3.804 \cdot 10^{-3}$
β_5		$4.212 \cdot 10^{-3}$	$2.295 \cdot 10^{-3}$
β_6			$3.439 \cdot 10^{-3}$

Table 3
γ values (in atomic units) of V_{Morse} for CD_4 with one and three deuteriums pointing towards the surface [see Eq. (8)].

one	three	value
$\gamma_{12}, \gamma_{22}, \gamma_{32}, \gamma_{42}$	$\gamma_{12}, \gamma_{22}, \gamma_{32}, \gamma_{42}$	$7.629 \cdot 10^{-3}$
$\gamma_{13}, -3\gamma_{23}, -3\gamma_{33}, -3\gamma_{43}$	$-\gamma_{13}, 3\gamma_{23}, 3\gamma_{33}, 3\gamma_{43}$	$1.397 \cdot 10^{-3}$
$\gamma_{14}, -3\gamma_{24}, -3\gamma_{34}, -3\gamma_{44}$	$-\gamma_{14}, 3\gamma_{24}, 3\gamma_{34}, 3\gamma_{44}$	$-1.454 \cdot 10^{-2}$
$\gamma_{17}, \gamma_{18}, \gamma_{19}, \gamma_{1,10}, \gamma_{28}, \gamma_{2,10}$	$\gamma_{17}, \gamma_{18}, \gamma_{19}, \gamma_{1,10}, \gamma_{28}, \gamma_{2,10}$	0.0
$\gamma_{27}, -2\gamma_{37}, -2\gamma_{47}$	$-\gamma_{27}, 2\gamma_{37}, 2\gamma_{47}$	$1.318 \cdot 10^{-3}$
$\gamma_{38}, -\gamma_{48}$	$\gamma_{38}, -\gamma_{48}$	$-1.114 \cdot 10^{-3}$
$\gamma_{29}, -2\gamma_{39}, -2\gamma_{49}$	$-\gamma_{29}, 2\gamma_{39}, 2\gamma_{49}$	$-1.371 \cdot 10^{-2}$
$\gamma_{3,10}, -\gamma_{4,10}$	$-\gamma_{3,10}, \gamma_{4,10}$	$1.187 \cdot 10^{-2}$

Table 4
γ values (in atomic units) of V_{Morse} for CD_4 with two deuteriums pointing towards the surface [see Eq. (8)].

two	value
$\gamma_{12}, \gamma_{22}, \gamma_{32}, \gamma_{42}$	$7.629 \cdot 10^{-3}$
$\gamma_{13}, \gamma_{23}, -\gamma_{33}, -\gamma_{43}, \gamma_{17}, -\gamma_{27}, \gamma_{37}, -\gamma_{47}, \gamma_{18}, -\gamma_{28}, -\gamma_{38}, \gamma_{48}$	$-8.070 \cdot 10^{-4}$
$\gamma_{14}, \gamma_{24}, -\gamma_{34}, -\gamma_{44}, \gamma_{19}, -\gamma_{29}, \gamma_{39}, -\gamma_{49}, \gamma_{1,10}, -\gamma_{2,10}, -\gamma_{3,10}, \gamma_{4,10}$	$8.396 \cdot 10^{-3}$

Table 5
Excitation probabilities at the surface, at an initial translational energy of 96 kJ/mol and all initial vibrational states in the ground state, for the intramolecular PES with elongation of the C–D bonds [see Eq. (12)] in the a_1 modes of the C_{3v} and C_{2v} symmetry, with one, two or three deuteriums pointing towards the surface. These modes are a $\nu_1(a_1)$ symmetrical stretch, a $\nu_2(e)$ bending, a $\nu_3(t_2)$ asymmetrical stretch, and a $\nu_4(t_2)$ umbrella. In parenthesis is the irreducible representation in T_d symmetry.

orientation	$\nu_1(a_1)$ stretch	$\nu_2(e)$ bending	$\nu_3(t_2)$ stretch	$\nu_4(t_2)$ umbrella
one	0.460		0.910	0.174
two	0.792	0.092	0.830	0.495
three	0.868		0.756	0.387

Table 6
Expectation values of the kinetic energy per mode in mHartree for CH_4 and CD_4, at an initial translational energy of 96 kJ/mol and all initial vibrational states in the ground state, for the intramolecular PES with elongation of the C–H/D bonds [see Eq. (12)] in the a_1 modes of the C_{3v} and C_{2v} symmetry, with one, two or three deuteriums pointing towards the surface. These modes are a $\nu_1(a_1)$ symmetrical stretch, a $\nu_2(e)$ bending , a $\nu_3(t_2)$ asymmetrical stretch, and a $\nu_4(t_2)$ umbrella. In parenthesis is the irreducible representation in T_d symmetry.

isotope	orientation	translation	$\nu_1(a_1)$ stretch	$\nu_2(e)$ bending	$\nu_3(t_2)$ stretch	$\nu_4(t_2)$ umbrella
CH_4	initial	36.57	3.30	1.75	3.39	1.50
	one	16.76	3.56		4.53	1.51
	two	14.59	3.50	1.79	4.67	1.57
	three	20.53	5.32		4.39	1.58
CD_4	initial	36.57	2.33	1.24	2.52	1.12
	one	16.17	2.61		4.09	1.18
	two	14.00	2.78	1.27	4.05	1.27
	three	20.06	4.37		3.80	1.28

Table 7
Expectation values of the potential energy terms in mHartree for CH_4 and CD_4, at an initial translational energy of 96 kJ/mol and all initial vibrational states in the ground state, for the intramolecular PES with elongation of the C–H/D bonds [see Eq. (12)]. $V_{\rm surf}$ is the total surface hydrogen repulsion; $V_{\rm harm}(\nu_2)$ and $V_{\rm harm}(\nu_4)$ are the harmonic terms of the intramolecular PES of the a_1 modes in the C_{3v} and C_{2v} symmetry corresponding to a $\nu_2(e)$ bending and $\nu_4(t_2)$ umbrella modes respectively in the T_d symmetry. $V_{\rm bond}(R_{\rm up})$ and $V_{\rm bond}(R_{\rm down})$ are the potential energy in a single C–H/D bond pointing respectively towards and away from the surface.

isotope	orientation	$V_{\rm surf}$	$V_{\rm harm}(\nu_2)$	$V_{\rm harm}(\nu_4)$	$V_{\rm bond}(R_{\rm up})$	$V_{\rm bond}(R_{\rm down})$
CH_4	initial	0.00	1.75	1.50	3.39	3.39
	one	18.20		1.87	3.25	3.85
	two	18.55	2.18	4.01	2.75	3.45
	three	9.22		2.94	3.00	3.74
CD_4	initial	0.00	1.24	1.12	2.48	2.48
	one	17.94		1.89	2.43	3.44
	two	18.45	1.68	4.52	2.29	2.74
	three	8.71		3.49	2.28	3.21